

Effects of the Size of Cosmological N-body Simulations on Physical Quantities – II: Halo Formation and Destruction Rate

Jayanti Prasad

Harish-Chandra Research Institute, Allahabad 211 019, India.

e-mail: jayanti@mri.ernet.in

Received 2007 February 22; accepted 2007 September 5

Abstract. In this study we show how errors due to finite box size affect formation and the destruction rate for haloes in cosmological N-body simulations. In an earlier study we gave an analytic prescription of finding the corrections in the mass function. Following the same approach, in this paper we give analytical expressions for corrections in the formation rate, destruction rate and the rate of change in comoving number density, and compute their expected values for the power law ($n = -2$) and LCDM models.

Key words. Large scale structure of Universe—N-body simulations—galaxies.

1. Introduction

In prevalent models of structure formation in the Universe, galaxies, clusters of galaxies and other large-scale structures are believed to have formed due to gravitational amplification of small perturbations (Peebles 1980; Padmanabhan 1993, 2002; Peacock 1999; Bernardeau *et al.* 2002). In cold dark matter dominated models these perturbations collapse hierarchically, i.e., smaller structures form first and then they merge and form larger structures.

In models of structure formation the main goal is to understand the growth of perturbations at various scales. It has been found that the linear perturbation theory closely follows the actual growth of perturbation at any scale as long as the amplitude of perturbation at that scale is small. However, the linear approximation breaks down once the amplitude becomes large because perturbations at various scales couple with each other and the system becomes nonlinear. Many approximations have been proposed (Zel'dovich 1970; Gurbatov *et al.* 1989; Saichev & Shandarin 1989; Matarrese *et al.* 1992; Brainerd *et al.* 1993; Hui & Bertschinger 1996; Bagla & Padmanabhan 1994; Sahni & Coles 1995) to explain nonlinear gravitational clustering but their validity has been limited to special cases. Cosmological N-body simulations are the main tools to understand gravitational clustering in nonlinear regime (Efstathiou *et al.* 1985; Bertschinger 1998; Bagla & Padmanabhan 1997a; Bagla 2005).

In N-body simulations we simulate a representative region of the universe which is in general large but finite. This restricts us from incorporating perturbations at scales greater than the size of the simulation box. We cannot also consider perturbations at

scales smaller than the grid length. This means that there is a natural truncation of power spectrum at large as well as small wave numbers. It has been shown in earlier studies (Peebles 1974, 1985; Little *et al.* 1991; Bagla & Padmanabhan 1997b) that the truncation of power spectrum at small scales does not affect large scale clustering in any significant way. However, significant effects of the truncation of power spectrum at large scales on clustering at small scales have been found (Gelb & Bertschinger 1994a, b; Bagla & Ray 2005; Power & Knebe 2006; Bagla & Prasad 2006, hereafter BP06).

Apart from N-body simulations, an analytical prescription given by Press & Schechter (1974) has been used to find mass function and related quantities. In this prescription, the fraction of mass in the collapsed objects having mass greater than a certain value, is identified with the fraction of volume in the initial density field which had density contrast, filtered over an appropriate scale, greater than a critical density contrast. The Press–Schechter formalism has been used in many studies to compute merging and mass function (Bond *et al.* 1991; Bower 1991; Lacey & Cole 1993, 1994; Sasaki 1994; Kitayama & Suto 1996; Cohn *et al.* 2001). In many of these studies, the main goal has been to test the results based on the Press–Schechter formalism against N-body simulations. Here our goal is to find the analytic corrections in the formation and destruction rate of haloes in N-body simulations due to finite box size of the simulation box.

The effects of the box size on the physical quantities in N-body simulations have been studied before. Gelb & Bertschinger (1994a) showed that the rms fluctuation in the mass and pairwise velocity dispersion at a given scale are underestimated when the size of the simulation box is reduced. Bagla & Ray (2005) computed the finite box effects on the average two-point correlation function, power spectrum and cumulative mass function in N-body simulations. They found that the required box size for simulating the LCDM model at high redshift is much larger than what people generally use. Power & Knebe (2006) studied the effects of box size on kinematical properties of cold dark matter haloes and concluded that the distribution of internal properties of haloes (like spin parameter) is not very sensitive to the box size. So far, most of the studies used N-body simulations for drawing their conclusions. In one of our earlier studies (BP06) we proposed an analytic prescription for estimating the corrections due to box size in N-body simulations for rms fluctuations in mass, two-point correlation function and the mass function.

The mass function is an important physical quantity in nonlinear gravitational clustering. It has been used to compare various theoretical models with observations (White *et al.* 1993; Ma & Bertschinger 1994; Ostriker & Steinhardt 1995; Bagla *et al.* 1996; White 2002). However, it does not contain all the information that is needed for various physical processes. For example, if we want to know the comoving number density of ionizing sources at any redshift then the mass function contains insufficient information since not all bound objects become the source of ionization, only those objects become ionizing sources which form during a particular period of time (Chiu & Ostriker 2000). In this situation we need to know the formation and destruction rate of collapsed objects as a function of redshift. The rate at which quasars form in the early universe depend in an important way on the merger rate which is another manifestation of the formation rate (Carlberg 1990). Apart from these there are many other cases like understanding the epoch of cluster formation etc., for which the formation and destruction rate of haloes are important (Bower 1991). In the present study we

carry forward our program and give analytic expressions for the corrections in the formation and destruction rate and estimate their values for the power law ($n = -2$) and LCDM models.

The plan of this paper is as follows. In section 2, we give the basic equations which are needed for our analysis. We give the expression for the clustering amplitude (rms fluctuations in mass), mass function and the rate of change in the comoving number density due to formation and destruction of haloes. In section 2.3, we show that the rate of change of comoving number density around a mass M can be written in terms of the rate at which the haloes of that mass are formed and the rate at which the haloes of that mass are destroyed due to merging. We present our results in section 3 and discuss their implications for the power law and LCDM models. In section 4 we summarize our results.

2. Basic equations

2.1 Clustering amplitude

In order to estimate the effects of box size on physical quantities in the linear regime, we use the mass variance $\sigma^2(r)$ (Peebles 1993; Peacock 1998; Padmanabhan 2002) as the base quantity.

$$\sigma^2(r) = 9 \int \frac{k^3 P(k)}{2\pi^2} \left(\frac{\sin kr - kr \cos kr}{k^3 r^3} \right)^2 \frac{dk}{k}. \quad (1)$$

On the basis of the correction in $\sigma^2(r)$, we find the corrections in other physical quantities. In BP06, we showed that the variance in mass is suppressed at all scales when we reduce the size of the simulation box. For example, if its actual value at scale r is $\sigma_0^2(r)$ then in the initial conditions of a simulation we obtain $\sigma^2(r, L_{\text{Box}})$ where:

$$\sigma^2(r, L_{\text{Box}}) = \sigma_0^2(r) - \sigma_1^2(r, L_{\text{Box}}). \quad (2)$$

Here L_{Box} is the size of the simulation box and $\sigma_1^2(r, L_{\text{Box}})$ is the correction due to the finite box size. Note that here $\sigma_1^2(r, L_{\text{Box}})$ is a positive quantity so clustering amplitude $\sigma^2(r)$ is always underestimated when we reduce the size of the simulation box.

2.2 Mass function and number density

In the Press–Schechter formalism, we consider the initial density field as Gaussian random and smooth it over a filter of size r (or mass M), then the fraction of mass in the collapsed objects $F(> M)$, having mass greater than M , at the final epoch, can be identified with the fraction of volume in the initial density field which had smoothed density contrast greater than some critical density contrast δ_c which is computed on the basis of the spherical collapse model.

$$F(> M, t) = \frac{2}{\sqrt{\pi}} \int_{\frac{\delta_c(t)}{\sqrt{2}\sigma(M)}}^{\infty} e^{-x^2} dx = \text{erfc} \left(\frac{\delta_c(t)}{\sqrt{2}\sigma(M)} \right). \quad (3)$$

The comoving number density $N_{PS}(M, t)dM$ of objects which have mass in the range $[M, M + dM]$ at time t is given by

$$\begin{aligned} N_{PS}(M, t)dM &= \frac{\rho_0}{M} \times \frac{dF(> M)}{dM} dM \\ &= \sqrt{\frac{2}{\pi}} \frac{\rho_0}{M} \left(-\frac{\delta_c(t)}{\sigma^2(M)} \frac{d\sigma(M)}{dM} \right) \exp\left(-\frac{\delta_c^2(t)}{2\sigma^2(M)}\right) dM. \end{aligned} \quad (4)$$

Here we can use $\delta_c(t) = \delta_c/D(t)$ where $D(t)$ is the linear growth factor which depends on the cosmological model being considered and $\delta_c(t)$ is taken to be 1.68 at the present epoch.

2.3 The rate of change of number density

We can find the rate of change in the comoving number density per unit time for objects which have mass in the range $[M, M + dM]$ from equation (4).

$$\begin{aligned} \left(\frac{dN_{PS}(M, t)}{dt} \right) dM &= \sqrt{\frac{2}{\pi}} \frac{\rho_0}{M} \left(\frac{1}{D^2(t)} \frac{dD(t)}{dt} \right) \left(\frac{\delta_c}{\sigma^2(M)} \frac{d\sigma(M)}{dt} \right) \\ &\quad \times \left[1 - \frac{\delta_c^2}{\sigma^2(M)D^2(t)} \right] \exp\left(-\frac{\delta_c^2}{2\sigma^2(M)D^2(t)}\right) dM. \end{aligned} \quad (5)$$

We can identify the first and second terms of the right-hand side with the destruction and formation rate respectively (Sasaki 1994; Kitayama & Suto 1996).

$$\begin{aligned} \left(\frac{dN_{PS}(M, t)}{dt} \right) dM &= -\frac{1}{D(t)} \frac{dD(t)}{dt} \left[1 - \frac{\delta_c^2}{\sigma^2(M)D^2(t)} \right] N_{PS}(M, t)dM \\ &= -\left(\frac{dN_{Dest}(M, t)}{dt} \right) dM + \left(\frac{dN_{Form}(M, t)}{dt} \right) dM. \end{aligned} \quad (6)$$

The formation rate $(dN_{Form}(M, t)/dt)dM$ quantifies the change in the comoving number density of objects around mass M , per unit time, due to the formation of objects in that mass range when objects of mass smaller than M merge together.

$$\begin{aligned} \left(\frac{dN_{Form}(M, t)}{dt} \right) dM &= \frac{1}{D(t)} \frac{dD(t)}{dt} \left[\frac{\delta_c^2}{\sigma^2(M)D^2(t)} \right] N_{PS}(M, t)dM \\ &= \sqrt{\frac{2}{\pi}} \frac{\rho_0}{M} \left(\frac{1}{D^4(t)} \frac{dD(t)}{dt} \right) \left(-\frac{\delta_c^3}{\sigma^4(M)} \frac{d\sigma(M)}{dt} \right) \\ &\quad \times \exp\left(-\frac{\delta_c^2}{2\sigma^2(M)D^2(t)}\right) dM. \end{aligned} \quad (7)$$

The destruction rate $(dN_{\text{Dest}}(M, t)/dt)dM$ quantifies the rate of change of comoving number density of haloes in the mass range $[M, M + dM]$ when the haloes in that mass range merge together and form bigger haloes.

$$\begin{aligned} \left(\frac{dN_{\text{Dest}}(M, t)}{dt}\right)dM &= \frac{1}{D(t)} \frac{dD(t)}{dt} N_{PS}(M, t)dM \\ &= \sqrt{\frac{2}{\pi}} \frac{\rho_0}{M} \left(\frac{1}{D^2(t)} \frac{dD(t)}{dt}\right) \left(-\frac{\delta_c}{\sigma^2(M)} \frac{d\sigma(M)}{dt}\right) dM \\ &\quad \times \exp\left(-\frac{\delta_c^2}{2\sigma^2(M)D^2(t)}\right) dM. \end{aligned} \quad (8)$$

3. Box corrections

On the basis of the correction due to finite box size in $\sigma^2(r)$ (equation (2)) we can find the corrections in the number density, the rate of change in the number density, the rate of formation and the rate of destruction, i.e., equations (4), (5), (7), and (8) respectively.

3.1 Corrections in comoving number density

On the basis of the Press–Schechter formalism the comoving number density of objects in a mass range around a mass scale can be related to the rms fluctuations in the mass at that scale. Using the technique which we have developed to compute the corrections due to finite box size in the rms fluctuations in mass (see equation (2)), we can find the corrections in the comoving number density also.

The comoving number density which we expect in cosmological N-body simulations is given by

$$\begin{aligned} N_{PS}(M, t)dM &= \sqrt{\frac{2}{\pi}} \frac{\rho_0}{M} \frac{\delta_c}{D(t)} \left(-\frac{1}{\sigma^2(M)} \frac{d\sigma(M)}{dM}\right) \\ &\quad \times \exp\left(-\frac{\delta_c^2}{2\sigma^2(M)D^2(t)}\right) dM \\ &= N_{PS,0}(M, t)dM - N_{PS,1}(M, t)dM. \end{aligned} \quad (9)$$

Here $N_{PS,0}(M, t)$ and $N_{PS}(M, t)$ are the theoretical (box size infinite) and the actual (box size finite) comoving number densities respectively.

$$\begin{aligned} N_{PS,0}(M, t)dM &= \sqrt{\frac{2}{\pi}} \frac{\rho_0}{M} \frac{\delta_c}{D(t)} \left(\frac{-1}{\sigma_0^2(M)} \frac{d\sigma_0(M)}{dM}\right) \\ &\quad \times \exp\left(\frac{-\delta_c^2}{2\sigma_0^2(M)D^2(t)}\right) dM \end{aligned} \quad (10)$$

and

$$N_{PS,1}(M, t)dM = \frac{1}{2} \left[1 - \left(1 - \frac{\sigma_1^2}{\sigma_0^2} \right)^{-3/2} \left(1 - \frac{d\sigma_1^2}{d\sigma_0^2} \right) \right. \\ \left. \times \exp \left\{ -\frac{\delta_c^2}{2D^2(t)} \left(\frac{1}{\sigma^2} - \frac{1}{\sigma_0^2} \right) \right\} \right] N_{PS,0}(M, t)dM \quad (11)$$

or

$$N_{PS,1}(M, t)dM \approx \frac{1}{2} \left[\frac{d\sigma_1^2}{d\sigma_0^2} - \frac{3\sigma_1^2}{2\sigma_0^2} + \frac{\delta_c^2 \sigma_1^2}{2D^2(t)\sigma_0^4} \right] N_{PS,0}(M, t)dM, \\ \text{if } \sigma_1^2/\sigma_0^2 < 1. \quad (12)$$

In equation (12) the coefficient of $N_{PS,0}(M, t)$ changes sign at the scale for which $\sigma_0 \approx \delta_c/D(t)\sqrt{3} = \delta_c(t)/\sqrt{3}$ so the number density of objects below this scale is overestimated and the number density above this scale is underestimated. This is in accordance with our earlier results (BP06).

Figure (1) shows the theoretical comoving number density $N_{PS,0}$ and the actual comoving number density N_{PS} , which we expect in an N-body simulation for the power law model ($n = -2$) at the present epoch ($z = 0$). In this case we consider a simulation box of size $128 h^{-1}\text{Mpc}$ and normalize the initial power spectrum such that

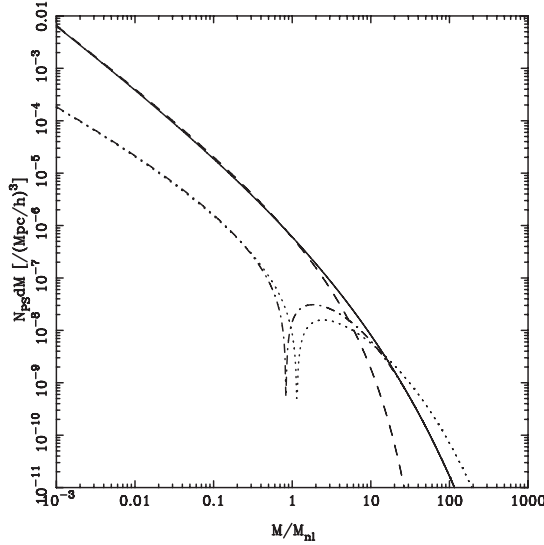


Figure 1. This figure shows the actual comoving number density $N_{PS,0}dM$ (solid line) and the comoving number density $N_{PS} dM$ (dashed line) which we expect in a cosmological N-body simulation at the present epoch ($z = 0$) for a power law ($n = -2$) model (see equations (9, 10)). Here we consider the size of the simulation box $128 h^{-1}\text{Mpc}$ and normalize the initial power spectrum such that the scale of non-linearity (r_{nl}) at $z = 0$ is $8 h^{-1}\text{Mpc}$. In the figure, the exact (dot-dashed line) and approximate (dotted line) corrections in the comoving number density due to finite box size are also shown (see equations (11, 12)).

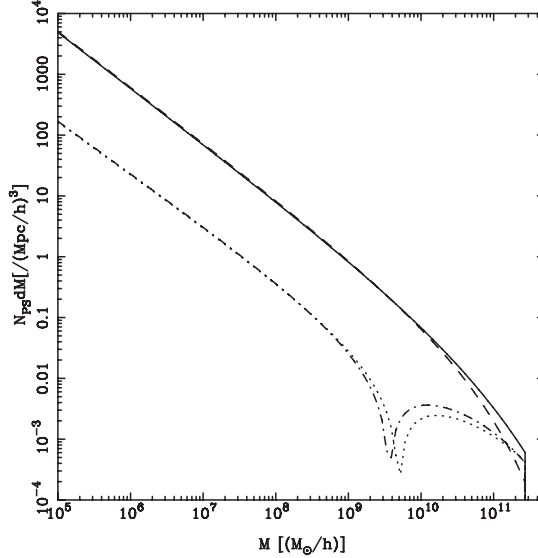


Figure 2. This figure shows the actual comoving number density $N_{PS,0} dM$ (solid line) and the comoving number density $N_{PS} dM$ (dashed line) which we expect in a cosmological N-body simulation for the LCDM model at $z = 6$ (see equations (9, 10)). Here the size of the simulation is taken to be $10 h^{-1} \text{Mpc}$. We have also shown the exact (dot-dashed line) and approximate (dotted line) corrections in the comoving number density due to finite box size (see equations (11, 12)).

the scale of non-linearity at $z = 0$ is $8 h^{-1} \text{Mpc}$. The actual and approximate corrections in the comoving number density are also shown in the figure. This figure shows that in N-body simulations the number density of large mass haloes is underestimated. However, it is overestimated for small mass haloes. This feature is more evident from the actual and approximate corrections (difference between the theoretical and actual values). In Fig. 2 we show the theoretical and the actual comoving number densities and corrections due to finite box size for the LCDM model. In this case we consider a simulation box of size $10 h^{-1} \text{Mpc}$ and compute physical quantities at $z = 6$. From Figs. 1 and 2 it is clear that the overall trend remains the same. This result is in agreement with the results of our earlier study (BP06).

3.2 Formation rate

The rate of formation of haloes of mass M which we expect in N-body simulation is given by equation (7)

$$\begin{aligned}
 \left(\frac{dN_{\text{Form}}(M, t)}{dt} \right) dM &= \sqrt{\frac{2}{\pi}} \frac{\rho_0}{M} \left(\frac{1}{D^4(t)} \frac{dD(t)}{dt} \right) \left(-\frac{\delta_c^3}{\sigma^4(M)} \frac{d\sigma(M)}{dt} \right) \\
 &\quad \times \exp \left(-\frac{\delta_c^2}{2\sigma^2(M)D^2(t)} \right) dM \\
 &= \left(\frac{dN_{\text{Form},0}(M, t)}{dt} \right) dM - \left(\frac{dN_{\text{Form},1}(M, t)}{dt} \right) dM. \quad (13)
 \end{aligned}$$

Here $(dN_{\text{Form},0}(M, t)/dt)dM$ and $(dN_{\text{Form},1}(M, t)/dt)dM$ are the theoretical formation rate and the correction term respectively.

$$\begin{aligned} \left(\frac{dN_{\text{Form},0}(M, t)}{dt}\right) dM &= \sqrt{\frac{2}{\pi}} \frac{\rho_0}{M} \left(\frac{1}{D^4(t)} \frac{dD(t)}{dt}\right) dM \\ &\times \left(-\frac{\delta_c^3}{\sigma_0^4(M)} \frac{d\sigma_0(M)}{dt}\right) \exp\left(-\frac{\delta_c^2}{2\sigma_0^2(M)D^2(t)}\right) \end{aligned} \quad (14)$$

and

$$\begin{aligned} \left(\frac{dN_{\text{Form},1}(M, t)}{dt}\right) dM &= \frac{1}{2} \left[1 - \left(1 - \frac{\sigma_1^2}{\sigma_0^2}\right)^{-5/2} \left(1 - \frac{d\sigma_1^2}{d\sigma_0^2}\right)\right. \\ &\times \left.\exp\left\{-\frac{\delta_c^2}{2D^2(t)} \left(\frac{1}{\sigma^2} - \frac{1}{\sigma_0^2}\right)\right\}\right] \left(\frac{dN_{\text{Form},0}(M, t)}{dt}\right) dM \end{aligned} \quad (15)$$

or

$$\begin{aligned} \left(\frac{dN_{\text{Form},1}(M, t)}{dt}\right) dM &\approx \frac{1}{2} \left[\frac{d\sigma_1^2}{d\sigma_0^2} - \frac{5\sigma_1^2}{2\sigma_0^2} + \frac{\delta_c^2\sigma_1^2}{2D^2(t)\sigma_0^4}\right] \\ &\times \left(\frac{dN_{\text{Form},0}(M, t)}{dt}\right) dM \quad \text{if } \sigma_1^2/\sigma_0^2 < 1. \end{aligned} \quad (16)$$

Figures 3 and 4 show the theoretical formation rate $(dN_{\text{Form},0}/dt)dM$ and the actual formation rate $(dN_{\text{Form}}/dt)dM$ for the power law and LCDM models respectively. The parameters for the power law and LCDM model are the same as in Figs. 1 and 2 respectively. Since the formation rate is directly proportional to the comoving number density, it follows the same trend as the comoving number density. However, in this case the scale at which the correction term changes sign is different from the scale at which the correction term for the comoving number density changes, i.e., here it is the scale for which $\sigma_0 = \delta_c/D(t)\sqrt{5} = \delta_c(t)/\sqrt{5}$. From these figures we see that the formation rate of massive haloes is suppressed. However, that of low mass haloes is enhanced in N-body simulations when the box size is reduced. The main reason behind the suppression of the formation of large mass haloes is the absence of fluctuations in the initial density field at large scales due to truncation of power.

3.3 Destruction rate

Following the same approach as we have applied for the formation rate, we can find the corrections due to finite box size for destruction rate, i.e., equation (8) also.

$$\left(\frac{dN_{\text{Dest}}(M, t)}{dt}\right) dM = \left(\frac{dN_{\text{Dest},0}(M, t)}{dt}\right) dM - \left(\frac{dN_{\text{Dest},1}(M, t)}{dt}\right) dM \quad (17)$$

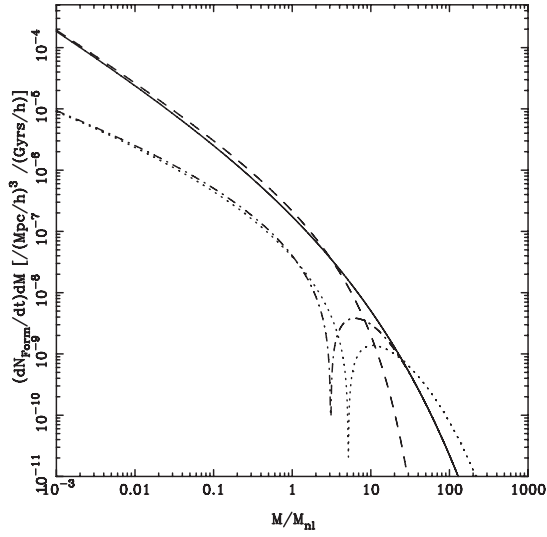


Figure 3. This figure shows the actual formation rate $(dN_{\text{Form},0}/dt)dM$ (solid line) and the formation rate $(dN_{\text{Form}}/dt)dM$ (dashed line) which we expect in a cosmological N-body simulation for the power law model (see equations (13, 14)). All the parameters for this figure are the same as for Fig. 1. We have also shown the exact (dot-dashed line) and approximate (dotted line) corrections in the formation rate due to finite box size (see equations (15, 16)).

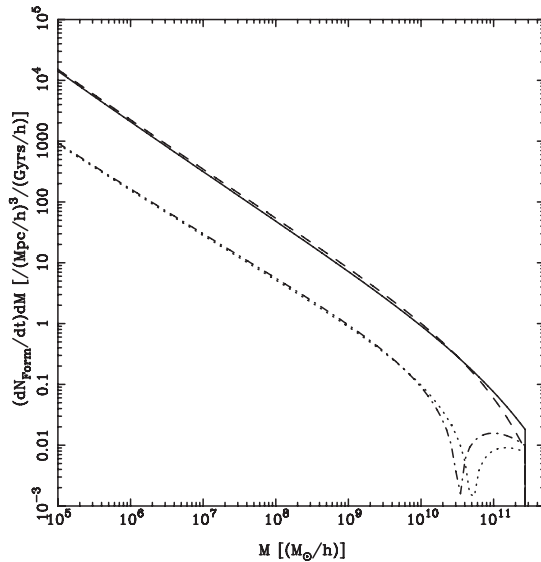


Figure 4. This figure shows the actual formation rate $(dN_{\text{Form},0}/dt)dM$ (solid line) and the formation rate $(dN_{\text{Form}}/dt)dM$ (dashed line) which we expect in a cosmological N-body simulation for the LCDM model (see equations (13, 14)). For this figure all the parameters are identical to that of Fig. 2. The exact (dot-dashed line) and approximate (dotted line) corrections in the formation rate due to finite box size are also shown (see equations (15, 16)).

where

$$\begin{aligned} \left(\frac{dN_{\text{Dest},0}(M, t)}{dt} \right) dM &= \sqrt{\frac{2}{\pi}} \frac{\rho_0}{M} \left(\frac{1}{D^2(t)} \frac{dD(t)}{dt} \right) \left(-\frac{\delta_c}{\sigma_0^2(M)} \frac{d\sigma_0(M)}{dt} \right) \\ &\quad \times dM \exp \left(-\frac{\delta_c^2}{2\sigma_0^2(M)D^2(t)} \right) \end{aligned} \quad (18)$$

and

$$\begin{aligned} \left(\frac{dN_{\text{Dest},1}(M, t)}{dt} \right) dM &= \frac{1}{2} \left[1 - \left(1 - \frac{\sigma_1^2}{\sigma_0^2} \right)^{-3/2} \left(1 - \frac{d\sigma_1^2}{d\sigma_0^2} \right) \right. \\ &\quad \left. \times \exp \left\{ -\frac{\delta_c^2}{2D^2(t)} \left(\frac{1}{\sigma^2} - \frac{1}{\sigma_0^2} \right) \right\} \right] \left(\frac{dN_{\text{Dest},0}(M, t)}{dt} \right) \end{aligned} \quad (19)$$

or

$$\begin{aligned} \left(\frac{dN_{\text{Dest},1}(M, t)}{dt} \right) dM &\approx \frac{1}{2} \left[\frac{d\sigma_1^2}{d\sigma_0^2} - \frac{3\sigma_1^2}{2\sigma_0^2} + \frac{\delta_c^2 \sigma_1^2}{2D^2(t)\sigma_0^4} \right] \\ &\quad \times \left(\frac{dN_{\text{Dest},0}(M, t)}{dt} \right) \quad \text{if } \sigma_1^2/\sigma_0^2 < 1. \end{aligned} \quad (20)$$

Figures 5 and 6 show the destruction rates for the power law and LCDM model respectively. The parameters for the power law and LCDM models are the same as in Figs. 1 and 2 respectively. In this case the correction term changes sign at the same scale at which the correction term for the comoving number density changes. This is because $N_{PS,1}/N_{PS,0}$ and $N_{\text{Dest},1}/N_{\text{Dest},0}$ are equal and so $N_{PS,1}$ and $N_{\text{Dest},1}$ have the same scale of zero crossing. Here also we find that the destruction rate for the massive haloes are suppressed. However, they are enhanced for the low mass haloes when we reduce the size of the simulation box.

3.4 Rate of change on number density

The rate of change of the number density is defined as (see equation (7))

$$\begin{aligned} \left(\frac{N_{PS}(M, t)}{dt} \right) dM &= \frac{-1}{D(t)} \frac{dD(t)}{dt} \left[1 - \frac{\delta_c^2}{\sigma^2(M)D^2(t)} \right] N_{PS}(M, t) dM \\ &= - \left(\frac{dN_{\text{Dest}}(M, t)}{dt} \right) dM + \left(\frac{dN_{\text{Form}}(M, t)}{dt} \right) dM. \end{aligned} \quad (21)$$

We have already given the corrections for the formation rate $(dN_{\text{Form}}/dt)dM$ and the destruction rate $(dN_{\text{Dest}}/dt)dM$ in the last two sections. The correction in the rate of change of number density $(dN_{PS}(M, t)/dt)dM$ can be written in terms of the correction in the formation and destruction rates. In Figs. 7 and 8 we show the rate

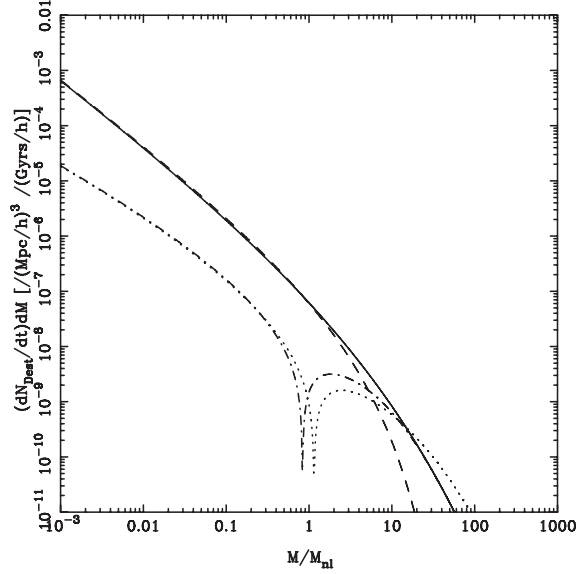


Figure 5. This figure shows the actual destruction rate $(dN_{\text{Dest},0}/dt)dM$ (solid line) and the formation rate $(dN_{\text{Dest}}/dt)dM$ (dashed line) which we expect in a cosmological N-body simulation (see equations (17, 18)) for the power law model. All the parameters for this figure are identical to that of Fig. 1. We have also shown the exact (dot-dashed line) and approximate (dotted line) corrections in the destruction rates due to finite box size (see equations (19, 20)).

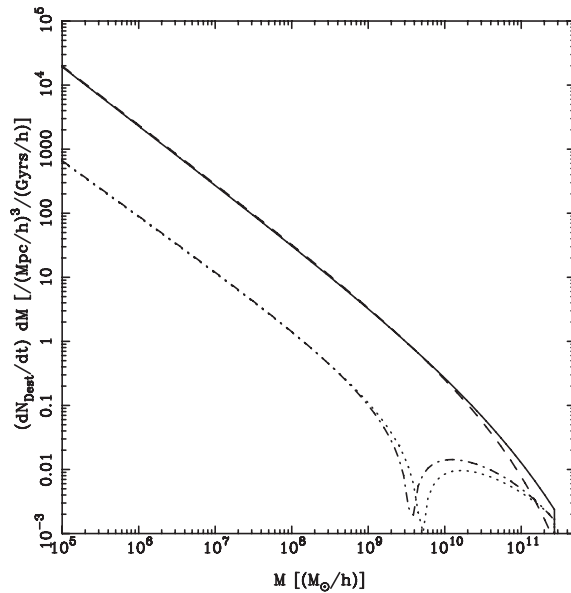


Figure 6. This figure shows the actual destruction rate $(dN_{\text{Dest},0}/dt)dM$ (solid line) and the formation rate $(dN_{\text{Dest}}/dt)dM$ (dashed line) which we expect in a cosmological N-body simulation (see equations (17, 18)) for the LCDM simulation. All the parameters for this figure are identical to that of Fig. 2. The exact (dot-dashed line) and approximate (dotted line) corrections in the destruction rate due to finite box size are also plotted (see equations (19, 20)).

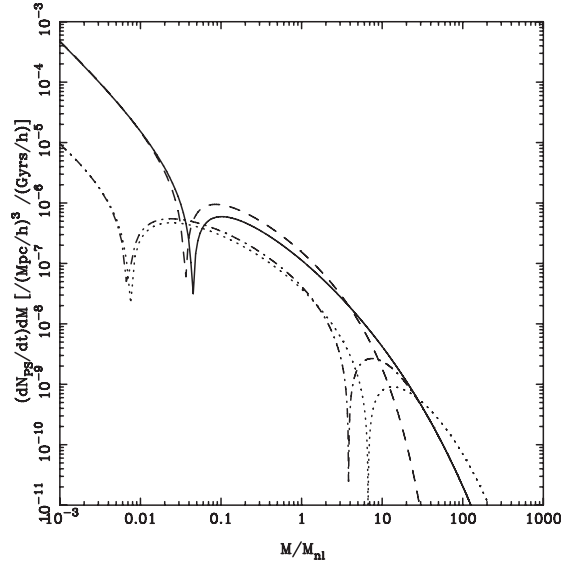


Figure 7. This figure shows the actual merger rate $(dN_{PS,0}/dt)dM$ (solid line) and the formation rate $(dN_{PS}/dt)dM$ (dashed line) which we expect in a cosmological N-body simulation for the power law ($n = -2$) (see equation (21)). All the parameters for this figure are the same as for Fig. 1. The exact (dot-dashed line) and approximate (dotted line) corrections in the rate of change in the comoving number density are also plotted.

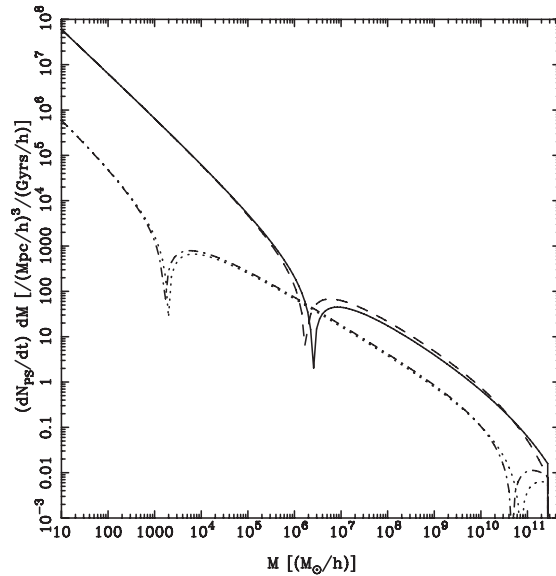


Figure 8. This figure shows the actual merger rate $(dN_{PS,0}/dt)dM$ (solid line) and the formation rate $(dN_{PS}/dt)dM$ (dashed line) which we expect in a cosmological N-body simulation for the LCDM model. All the parameters for this figure are the same as for Fig. 2. The exact (dot-dashed line) and approximate (dotted line) corrections in the rate of change in the comoving number density are also plotted.

of change of the comoving number density and the exact and approximate correction terms in it for the power law and LCDM model respectively. From equation (21) it is clear that for $\sigma(M) < \delta_c/D(t)$ the rate of change of number density \dot{N}_{PS} is dominated by the formation rate, and for $\sigma(M) > \delta_c/D(t)$ by the destruction rate. For any time t , we can find a mass scale M_c for which $\sigma(M_c) = \delta_c/D(t)$, i.e., the formation and the destruction rate are equal and so there is no net change in the comoving number density of objects at that scale. In hierarchical clustering models, i.e., $\sigma(M)$ is a decreasing function of mass, comoving number density at large scales mainly changes due to the formation of massive haloes and at small scales due to destruction of smaller haloes.

The rate of change in the number density is underestimated at large and small scales, however, it is overestimated at intermediate scales. This feature is clear from Fig. 7 in which the actual and approximate error terms are positive at large and small scales but they are negative at intermediate scales and we have two zeroes crossing.

4. Discussion

In the hierarchical clustering models of structure formation, formation and destruction of haloes is a common process. In the present study we have shown that the formation and destruction rate of haloes due to gravitational clustering are affected significantly if the size of the simulation box is not sufficiently large. On the basis of the Press–Schechter formalism we have given the analytic expressions for the corrections in the comoving number density, formation rate, destruction rate and the rate of change in the number density of haloes at a given mass scale. We have considered the implications of our analysis for the power law ($n = -2$) and LCDM models. Since the box corrections are more important for models which have significant power at large scales, most of the models in which there is none or very less power at large scales are not affected by the size of the simulation box. However, models in which there is a lot of power at large scales (n is large and negative) the box effects can be quite large. In both the cases, i.e., power law and LCDM models, the scales at which we have shown the corrections are far below the size of the simulation box.

The main conclusions of the present study are as follows:

- If the size of the simulation box in N -body simulations is not large enough then the clustering amplitude is underestimated at all scales.
- At any given time, there is a scale above which merging is dominated by the formation rate and below which it is dominated by the destruction rate.
- The comoving number density of haloes is underestimated at large scales and overestimated at small scales when we reduce the size of the simulation box.
- The formation and destruction rate also get modified by reducing the size of the simulation box. Particularly, they are underestimated at large scales and overestimated at small scales.
- The suppression of the formation rate as well as destruction rate at large scales is mainly due to the absence of fluctuations in the initial density field at large scales due to limitation of box size.
- In N -body simulations which have small power at large scales the corrections due to box size can be ignored.

Observations suggest that cosmological perturbations were present at all scales in the initial density field that have been probed. Particularly in dark matter models

(Diemand *et al.* 2005, 2006) the index of the power spectrum at small scales becomes close to -3 . So in order to simulate these models one has to be very careful in choosing the size of the simulation box. This is because if the index of power spectrum is close to -3 at the box scale also or if the scale of non-linearity is close to the size of the simulation box then the results can be significantly affected by the finite box effects.

In this and Bagla & Prasad (2006) we have presented our analytic results for taking into account the effects of finite box size on the mass function, formation and destruction rate and other physical quantities. In the next paper of this series we will present a detailed comparison of our analytic results with a set of cosmological N-body simulations of different box sizes.

Acknowledgements

I would like to thank Jasjeet Bagla for insightful comments and discussions. Numerical work for this study was carried out at cluster computing facilities at the Harish-Chandra Research Institute (<http://www.cluster.mri.ernet.in>). This research has made use of NASA's Astrophysical Data System.

References

- Bagla, J. S., Padmanabhan, T. 1994, *MNRAS*, **266**, 227.
 Bagla, J. S., Padmanabhan, T. 1997a, *Pramana*, **49** 161.
 Bagla, J. S., Padmanabhan, T. 1997b, *MNRAS*, **286**, 1023.
 Bagla, J. S., Padmanabhan, T., Narlikar, J. V. 1996, *Comments on Astrophysics*, **18**, 275.
 Bagla, J. S., Ray, S. 2005, *MNRAS*, **358**, 1076.
 Bagla, J. S., Prasad, J. 2006, *MNRAS*, **370**, 993.
 Bagla, J. S. 2005, *CSci*, **88**, 1088.
 Bernardeau, F., Colombi, S., Gaztanaga, R., Scoccimarro, R. 2002, *Phys. Rep.*, **367**, 1.
 Bertschinger, E. 1998, *ARA&A*, **36**, 599.
 Bond, J. R., Cole, S., Efstathiou, G., Kaiser, N. 1991, *ApJ*, **379**, 440.
 Bower, R. G. 1991, *MNRAS*, **248**, 332.
 Brainerd, T. G., Scherre R. J., Villumsen J. V. 1993, *ApJ*, **418**, 570.
 Carlberg, R. G. 1993, *ApJ*, **350**, 505.
 Chiu, W. A., Ostriker, J. P. 2000, *ApJ*, **534**, 507.
 Cohn, J. D., Bagla, J. S., White, M. 2001, *MNRAS*, **325**, 1053.
 Diemand, J., Moore, B., Stadel, J. 2005, *Nature*, **433**, 389.
 Diemand, J., Kuhlen, M., Madau, P. 2006, *ApJ*, **649**, 1.
 Efstathiou, G.; Davis, M.; White, S. D. M.; Frenk, C. S. 1985, *ApJ*, **57**, 241.
 Gelb, J. M., Bertschinger, E. 1994a, *ApJ*, **436**, 467.
 Gelb, J. M., Bertschinger, E. 1994b, *ApJ*, **436**, 491.
 Gurbatov, S. N., Saichev, A. I., Shandarin, S.F. 1989, *MNRAS*, **236**, 385.
 Hui, L., Bertschinger, E. 1996, *ApJ*, **471**, 1.
 Kitayama, T., Suto, Y. 1996, *MNRAS*, **280**, 638.
 Lacey, C., Cole, S. 1993, *MNRAS*, **262**, 627.
 Lacey, C., Cole, S. 1994, *MNRAS*, **271**, 676.
 Little, B., Weinberg, D. H., Park, C. 1991, *MNRAS*, **253**, 295.
 Ma, C.-P., Bertschinger, E. 1994, *ApJ*, **434L**, 5.
 Matarrese, S., Lucchin, F., Moscardini, L., Saez, D. 1992, *MNRAS*, **259**, 437.
 Ostriker, J. P., Steinhardt, P. J. 1995, *Nature*, **377**, 600.
 Padmanabhan, T. 1993, *Structure Formation in the Universe*, Cambridge University Press.
 Padmanabhan, T. 2002, *Theoretical Astrophysics, Volume III: Galaxies and Cosmology*, Cambridge University Press.
 Peacock, J. A. 1999, *Cosmological Physics*, Cambridge University Press.

- Peebles, P. J. E. 1974, *A&A*, **32**, 391.
Peebles, P. J. E. 1980, *The large-scale structure of the universe*, Princeton University Press.
Peebles, P. J. E. 1985, *Apj*, **297**, 350.
Power, C., Knebe, A. 2006 *MNRAS*, **370**, 691.
Press, W. H., Schechter, P. 1974, *ApJ*, **187**, 425.
Sahni, V., Coles, P. 1995, *Phys. Rep.*, **262**, 1.
Sasaki, S. 1994, *Publ. Astron. Soc. Japan*, **46**, 427.
White, M. 2002, *ApJS*, **143**, 241.
White, S. D. M., Efstathiou, G., Frenk, C. S. 1993, *MNRAS*, **262**, 1023.
Zel'dovich, Ya B. 1970, *A&A*, **5**, 84.